Probing the Structure of Supported Membranes and Tethered Oligonucleotides by Fluorescence Interference Contrast Microscopy

Caroline M. Ajo-Franklin, Chiaki Yoshina-Ishii, and Steven G. Boxer*

Department of Chemistry, Stanford University, Stanford, California 94305-5080

Received December 20, 2004. In Final Form: March 29, 2005

Fluorescence interference contrast microscopy (FLIC) is a powerful method to structurally characterize fluorescent objects with nanometer-scale resolution in the *z* direction. Here we use FLIC to characterize the water layer underlying supported membranes and membrane-tethered double-stranded oligonucleotides. FLIC measurements of supported membranes containing the lipid-anchored fluorescent dye DiI in both leaflets indicate the thickness of the water layer separating the solid support and the lower lipid leaflet is 1.3 ± 0.2 nm. Addition of cobalt(II) chloride to a DiI-supported membrane quenches the fluorescence in the top leaflet of the supported membrane; FLIC measurements of this system precisely locate the DiI to the bottom leaflet. These experiments confirm the accuracy of the model and parameters used to determine the water layer thickness, demonstrate the ability to differentiate between fluorescent objects whose average position differs by ∼1.9 nm, and provide a widely applicable method to test the resolution of other high-*z*-resolution fluorescent microscopies. FLIC measurements of Alexa-labeled double-stranded oligonucleotides tethered to a supported membrane indicate that the DNA double helix is oriented perpendicular to the surface. Complications that arise from uncertainly in the orientation of the fluorophore are discussed. Several improvements in FLIC methodology are described. These stringent tests of the resolution of FLIC and the ability to unambiguously determine fluorescent lipid distribution provide structural insight on assemblies at membrane interfaces and permit the detection of even subtle changes at such interfaces.

Introduction

Supported membranes have found wide applications as mimics of cell membranes[1−3] and in studies of the phase behavior of multicomponent lipid membranes.[4−6] Supported membranes are formed by self-assembly of lipid bilayers onto a solid support, typically silica (see Figure 1A). A thin water layer separates the bottom leaflet of the supported membrane from the glass or silica support; different reports[7−10] suggest that this layer is between 0.2 and 4 nm in thickness. Importantly, the lipids in supported membranes maintain the lateral fluidity associated with lipid membranes in vesicles and cells. The water layer separating the supported membrane from the solid support is believed to be critical for the lateral fluidity of both leaflets. Ideally, transmembrane proteins in supported membranes would show similar mobility; however, in the few studies reported, transmembrane proteins have been found to be largely immobile, at least on the length scale sampled by fluorescence recovery after photobleaching (FRAP) measurements.[11,12] Because transmembrane pro-

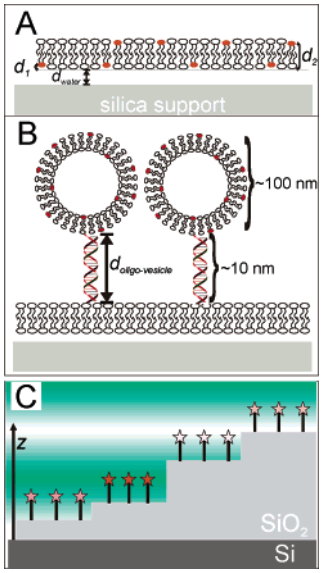

Figure 1. (A) Schematic diagram of a supported membrane. The position of fluorophores in the bottom and top leaflet relative to the aqueous layer is described by d_1 and d_2, respectively. (B) Schematic diagram of oligonucleotide-tethered vesicles. This diagram is not to scale; the approximate sizes of the oligonucleotide tether and the vesicle diameter are indicated. (C) Schematic diagram of the FLIC experiment. To determine the distance between a fluorescent object and the SiO_2 surface, identical objects are assembled on SiO_2 steps of different thicknesses on Si. The Si surface acts as mirror so that the incoming and reflected excitation light interfere, creating a standing wave of excitation light near the surface. Thus, the identical objects experience different light intensities on different SiO_2 steps. Although it is not shown for simplicity, the emitted fluorescence undergoes interference in a similar manner. For simplicity, the transition between SiO_2 steps is shown to be abrupt; however, this transition region between SiO_2 steps is actually quite gradual, with a slope of ∼1.

* Author to whom correspondence should be addressed. E-mail: sboxer@stanford.edu.

(1) Grakoui, A.; Bromley, S. K.; Sumen, C.; Davis, M. M.; Shaw, A. S.; Allen, P. M.; Dustin, M. L. *Science* **1999**, *285*, 221.
(2) Kloboucek, A.; Behrisch, A.; Faix, J.; Sackmann, E. *Biophys. J.* **1999**, *77*, 2311.
(3) Groves, J. T.; Dustin, M. L. *J. Immunol. Methods* **2003**, *278*, 19.
(4) Dietrich, C.; Bagatolli, L.; Volovyk, Z.; Thompson, N.; Levi, M.; Jacobson, K.; Gratton, E. *Biophys. J.* **2001**, *80*, 1417.
(5) Silvius, J. R. *Biochim. Biophys. Acta* **2003**, *1610*, 174.
(6) Crane, J. M.; Tamm, L. K. *Biophys. J.* **2004**, *86*, 2965.
(7) Bayerl, T. M.; Bloom, M. *Biophys. J.* **1990**, *58*, 357.
(8) Johnson, S. J.; Bayerl, T. M.; McDermott, D. C.; Adam, G. W. *Biophys. J.* **1991**, *59*, 289.
(9) Koenig, B. W.; Kruger, S.; Orts, W. J.; Majkrzak, C. F. *Langmuir* **1996**, *12*, 1343.
(10) Kiessling, V.; Tamm, L. K. *Biophys. J.* **2003**, *84*, 408.
(11) Salafsky, J.; Groves, J. T.; Boxer, S. G. *Biochemistry* **1996**, *35*, 14773.
(12) Wagner, M. L.; Tamm, L. K. *Biophys. J.* **2000**, *79*, 1400.

10.1021/la0468388 CCC: $30.25
Published on Web 04/28/2005

teins often have soluble domains which protrude from the membrane, the immobility of transmembrane proteins is frequently attributed to contact of the protein with the solid support.[11] It is often found that function is reduced or eliminated in immobile proteins; therefore, this poses severe restrictions in using supported membrane as a model system for studying transmembrane protein function in this format. To overcome these limitations, many investigators have attempted to separate the membrane from the solid support by a greater distance by tethering the membrane to the surface using spacers of fixed length or by incorporation of a polymer[10,12,13] or protein layer[14] to provide a cushion between the solid support and the membrane.

A different and promising approach to study interactions of membrane proteins in a nativelike environment utilizes two-dimensional arrays of vesicles tethered to the surface of a fluid-supported membrane by hybridization of complementary oligonucleotides (Figure 1B),[15] by chelation of oligohistidine by nickel nitrilotriacetic acid,[16] or by biotin–streptavidin coupling.[17–19] In the system developed in our lab,[15] small unilamellar vesicles displaying a short antisense oligonucleotide are exposed to a supported membrane that displays the sense oligonucleotides on its surface, resulting in tethering of intact and mobile vesicles in a sequence-specific manner to the supported membrane. Because it is straightforward to incorporate integral membrane proteins into vesicles and because the oligonucleotide-tethered vesicles are mobile and can be individually visualized, this system is potentially well suited for studying interactions between transmembrane proteins in different vesicles displaced from the solid support but retaining many of the advantages of the planar format.

For both supported membranes and oligonucleotide-tethered vesicles, the separation between the membrane surface including transmembrane proteins and nearest surface is presumed to dictate whether membrane components are mobile or not. For supported membranes, this distance corresponds to the water layer thickness, schematically illustrated as d_{water} in Figure 1A. For oligonucleotide-tethered vesicles, this distance is the shortest distance from the vesicle to the supported membrane, shown as $d_{oligo-vesicle}$ in Figure 1B. To gain insight into what forces modulate these separations—ultimately so that they can be controlled—measuring d_{water} and $d_{oligo-vesicle}$ with high precision is desirable. In addition to the value of more precisely measuring the water layer underlying supported membranes, greater precision would allow us to ask whether the water layer thickness is invariant or can be tuned by other parameters, such as lipid charge, ionic strength, and pH. In the same vein, we would like to characterize the distance separating tethered vesicles from the supported membrane. Because the persistence length of double-stranded DNA is many times larger than the length of the oligonucleotides used in the tethered vesicle system, the double-stranded oligonucleotide acts as a rigid rod, yet the linker which connects the lipid headgroup to the 5′ end of the sense strand has the potential to be quite flexibile. Knowledge of $d_{oligo-vesicle}$ would serve to additionally characterize the system of oligonucleotide-tethered vesicles, would suggest if significant interactions may be present between membrane components of the supporting membrane and the oligonucleotides or tethered vesicle and would inform interpretations of vesicle–vesicle interactions.

Measurements of d_{water} and $d_{oligo-vesicle}$ both require high precision information on the structure in the direction perpendicular to the surface, the z direction. Fluorescence interference contrast microscopy (FLIC), developed extensively by Fromherz and co-workers for biological microscopy,[20–22] uses a relatively simple experimental setup to attain high-resolution z information. To date, FLIC has been very effective in studies of biomimetic membranes, such as DiI-labeled cell membranes,[20–22] lipid components in tethered supported membranes,[10] and intermembrane junctions between a membrane patch and a supported membrane.[23–25] In FLIC (Figure 1C), the sample is assembled on a series of SiO_2 steps of different thickness on a highly reflective and flat Si surface, a FLIC chip. As shown schematically in Figure 1C, when a sample is imaged using a conventional epi-fluorescence microscope, interference between incoming and reflected excitation light creates a very well-defined variation in the excitation intensity in z. The emitted fluorescence interferes in a similar manner, and the different SiO_2 step thicknesses modulate the position of the fluorescent molecules relative to the overall interference pattern. Thus, the position of the fluorophore relative to the SiO_2 surface can be determined by fitting the observed fluorescence intensity as a function of the SiO_2 thickness to an appropriate model. In general, as the distance of the object from the SiO_2 surface increases, the maximum fluorescence intensity occurs at a smaller SiO_2 thickness. An analysis by Braun and Fromherz estimates the accuracy of FLIC to be ~1 nm;[21] however, this estimation assumes the distribution of fluorophores between the leaflets of the bilayer is known. Without such knowledge, distances determined by FLIC potentially have an additional systematic error of as much as ±1.8 nm.

The major drawback to FLIC is that the structure of interest must be assembled identically over all the SiO_2 steps.[26] Fortunately, this requirement poses no difficulty for supported membrane samples. However, this requirement poses a severe restriction for a population of oligonucleotides-tethered vesicles because the vesicle radius distribution typically has a standard deviation of ~20 nm. An alternative approach to measuring $d_{oligo-vesicle}$ is to replace the vesicle with a single fluorescent probe and to measure the corresponding separation. This is accomplished by hybridizing antisense oligonucleotides that are fluorescently labeled at the 5′ end to the sense oligonucleotides displayed by the supported membrane.

In the following, we use FLIC to characterize the water layer of supported membranes. Others[10] have previously measured the water layer thickness using FLIC by assuming that the fluorophores are equally distributed

(13) Sinner, E. K.; Knoll, W. *Curr. Opin. Chem. Biol.* **2001**, *5*, 705.
(14) Schuster, B.; Weigert, S.; Pum, D.; Sara, M.; Sleytr, U. B. *Langmuir* **2003**, *19*, 2392.
(15) Yoshina-Ishii, C.; Boxer, S. G. *J. Am. Chem. Soc.* **2003**, *125*, 3696.
(16) Stora, T.; Dienes, Z.; Vogel, H.; Duschl, C. *Langmuir* **2000**, *16*, 5471.
(17) Boukobza, E.; Sonnenfeld, A.; Haran, G. *J. Phys. Chem. B* **2001**, *105*, 12165.
(18) Jung, L. S.; Shumaker-Parry, J. S.; Campbell, C. T.; Yee, S. S.; Gelb, M. H. *J. Am. Chem. Soc.* **2002**, *122*, 4177.
(19) Stamou, D.; Duschl, C.; Delamarche, E.; Vogel, H. *Angew. Chem., Int. Ed.* **2003**, *42*, 5580.
(20) Lambacher, A.; Fromherz, P. *Appl. Phys. A* **1996**, *63*, 207.
(21) Braun, D.; Fromherz, P. *Appl. Phys. A* **1997**, *65*, 341.
(22) Lambacher, A.; Fromherz, P. *J. Opt. Soc. Am. B: Opt. Phys.* **2002**, *19*, 1453.
(23) Wong, A. P.; Groves, J. T. *J. Am. Chem. Soc.* **2001**, *123*, 12414.
(24) Parthasarathy, R.; Jackson, B. L.; Lowery, T. J.; Wong, A. P.; Groves, J. T. *J. Phys. Chem. B* **2004**, *108*, 649.
(25) Parthasarathy, R.; Groves, J. T. *Proc. Natl. Acad. Sci. U.S.A.* **2004**, *101*, 12798.
(26) Spatial variations in z on a single SiO_2 step can be seen as differences in fluorescence; however, additional information indicating the direction of these height fluctuations is necessary to obtain the absolute z position.[23–25]

between the two leaflets. We improve the accuracy of this measurement by explicitly measuring and accounting for the fluorophore distribution between the two leaflets. We present a stringent test of the ability of FLIC to distinguish small changes in position by comparing measurements of a supported membrane with fluorophores in both leaflets versus one containing fluorescent species only in the lower leaflet. To increase the precision of our measurement, we avoid contributions of inhomogeneous illumination and use a smaller NA objective to increase the sharpness of the interference pattern. These results quantitatively demonstrate the ability to resolve objects whose average position is 1.9 nm apart in the z direction, and thus provide a versatile resolution test that can be applied to other high-z-resolution fluorescent microscopy techniques. We also present FLIC results for fluorescently labeled double-stranded oligonucleotide tethers that suggest the distal end of the oligonucleotide tether is separated from the supported membrane by close to the maximal amount.

Materials and Methods

Fabrication and Characterization of FLIC Chips. FLIC chips, composed of a series of 16 SiO_2 steps on Si, were fabricated by standard photolithographic procedures. After RCA (Radio Corporation of America) cleaning, an approximately 150 nm thick layer of SiO_2 was grown on Si using thermal oxidation in the presence of O_2(g). Four rounds of photoresist development and buffered HF etching were used to produce 16 5 mm × 5 mm SiO_2 steps. A transparency mask was used to mask exposure of the photoresist; this relatively low-resolution mask created patterned borders between SiO_2 steps. For each round of etching, the HF concentration and etch time were adjusted to match the desired depth of etching. Before use, the FLIC chips were soaked in 90 °C 7x ICN detergent (diluted 1:5 in Millipore water, ICN Pharmaceuticals, Costa Mesa, CA), rinsed extensively in double distilled water, and baked at 400 °C for 4 h. After use, the FLIC chips were sonicated in water, 2-propanol, and chloroform, cleaned in piranha solution (75 vol% concentrated H_2SO_4 and 25 vol% 30% H_2O_2, heated to 70 °C), and the SiO_2 thickness for each step was measured by ellipsometry (Variable Angle Stokes Ellipsometer L116SF, Gaertner Scientific, Stokie, IL). The parameters $n_{Si} = 3.882$, $\kappa_{Si} = -0.019$ at 632.8 nm were used to determine the SiO_2 thickness. Unlike bulk SiO_2, ultrathin layers of SiO_2 less than 15 nm have a refractive index that depends on the SiO_2 thickness;[27−29] therefore, both the SiO_2 thickness and the SiO_2 refractive index were free parameters which were fit by the software. The resulting best-fit values of the SiO_2 refractive index as a function of SiO_2 thickness were consistent with values reported by Kalnitsky et al.[27] Ellipsometric measurements of the SiO_2 thickness were made at three locations on each step, with a resulting variation in thickness on the order of ±0.3 nm.

Formation and Imaging of Supported Bilayers. Small unilamellar vesicles composed of 0.5 mol% 1,1′-dioctadecyl-3,3,3′,3′-tetramethylindocarbocyanine (DiI, Molecular Probes, Eugene, OR) and 99.5 mol% egg phosphatidylcholine (egg PC, Avanti Polar Lipids, Alabaster, AL) were prepared in Millipore water (resistivity 18.2 MΩ/cm) by vesicle extrusion through 50 nm polycarbonate membranes. These vesicles were diluted to ~1 mg/mL in 10 mM phosphate 50 mM sodium chloride, pH 7.2 buffer immediately before use. Sulfhydryl-reactive vesicles composed of egg PC and 0.5 mol% 1,2-dipalmitoyl-*sn*-glycero-3-phosphoethanolamine-*N*-[3-(2-pyridyldithio)propionate] (N-PDP-PE, Avanti Polar Lipids, Alabaster, AL) were prepared at a lipid concentration of 25 mM in a 100 mM borate, 50 mM citrate, 100 mM sodium chloride, 2 mM EDTA, pH 8.0 buffer (borate−citrate buffer) by vesicle extrusion through 50 nm polycarbonate membranes. To prepare oligonucleotide-modified vesicles, the sense oligonucleotide (5′-AGCGGATAACAATTTCACACAGGA-3′) modified with a disulfide group on the 5′ end (C_6 thiol modification, IDT DNA Technologies, Coralville, IA) was exposed to 10 molar excess tris(2-carboxyethyl)phosphine (TCEP) and added to the sulfhydryl-reactive vesicles to a final DNA concentration of 50 μM. The resulting vesicles were isolated on a Sepharose CL-4B gel filtration column with the borate−citrate buffer as eluant.

To prepare Alexa 594-labeled antisense oligonucleotides, the antisense oligonucleotide (5′-TCCTGTGTGAAATTGTTATC-CGCT-3′) modified with a disulfide group on the 5′ end (C_6 thiol modification, IDT DNA Technologies, Coralville, IA) was dissolved in 20 mM phosphate 140 mM sodium chloride, pH 7.2 buffer, exposed to 10 molar excess TCEP, and added to 13 molar excess Alexa Fluor 594 C_5 maleimide (Molecular Probes, Eugene, OR) dissolved in dimethyl sulfoxide to a final oligonucleotide concentration of 0.1 mM. The Alexa-labeled oligonucleotides were isolated from the excess Alexa 594 C_5 maleimide using a standard ethanol precipitation with extensive washing. On the basis of the absorption spectrum and their extinction coefficients, the molar ratio of Alexa to oligonucleotide was 1:1.

The supported membranes were formed by vesicle fusion onto the FLIC chip, followed by extensive rinsing with Millipore water. For the FLIC experiments on Alexa-labeled oligonucleotide tethers, a solution of 0.5 nM Alexa-labeled antisense oligonucleotide in borate−citrate buffer was incubated with the supported membrane displaying the sense oligonucleotide for 30 min followed by extensive rinsing of the surface with additional buffer. Two small strips of double-sided tape were used to seal the FLIC chip-supported membrane to a 22 mm × 40 mm glass coverslip (~0.1 μm thickness), trapping an approximately 100 μm thick bulk water layer. This configuration, designed to eliminate lateral interference fringes created by reflection from the top glass coverslip and the FLIC chip, could also be used as a simple flow cell.

The FLIC images were acquired by imaging through the glass coverslip and water layer with a 0.45 NA 10× objective. A high-pressure mercury arc lamp (102DH, Ushio, Cypress CA) was used as the light source; images were acquired with a 16-bit CCD (Cascade 650S, Roper Scientific, Tucson, AZ) using a Texas Red filter set (HQ565/55x, Q595LP, and HQ645/75m, Chroma Technology, Brattleboro, VT) mounted in a Nikon TE200 microscope (Nikon USA, Melville NY). To eliminate differential contributions from inhomogeneous illumination across the field of view, the average background-corrected intensity at a given region within the field of view was calculated for each SiO_2 thickness using images taken at three different locations on a step. This average and its corresponding standard deviation are the reported values in Figures 3−5. The image shown in Figure 3B was linearly contrast-adjusted using Adobe PhotoShop.

Quenching by Cobalt(II) Chloride. To determine the fraction of DiI in the top lipid leaflet of a supported membrane, we performed fluorescence-quenching studies of DiI in supported membranes.[30] As additional controls, similar fluorescence quenching experiments were performed on DiI-containing supported monolayers, micelles, and vesicles in solution. Micelles containing DiI were formed by addition of *N*-*N*-dimethyldodecylamine-*N*-oxide (LDAO) to DiI-containing vesicles to ~1 vol%. Supported monolayers containing DiI were formed by vesicle fusion onto poly(dimethylsiloxane).[31] For quenching experiments on supported membranes and supported monolayers, the fluorescence intensity was measured by fluorescence microscopy before and after the addition of 500 mM cobalt(II) chloride to the bulk aqueous phase with exposure conditions that produced negligible photobleaching. The addition of cobalt(II) chloride did not change the background fluorescence intensity, and upon replacement of the cobalt(II) chloride solution with Millipore water, the fluorescence intensity returned to its initial level. For quenching experiments of DiI containing vesicles and micelles, the steady-state fluorescence of DiI in the presence of cobalt(II) chloride was compared to the same concentration of DiI (~25 nM) in vesicles or micelles in the absence of cobalt(II) chloride using a Spex Fluorolog 2 fluorimeter (Jobin Yvon, Edison, NJ).

Numerical Fitting, Modeling, and Parameters. To quantitatively model and fit FLIC data, Fromherz and co-workers

(27) Kalnitsky, A.; Tay, S. P.; Ellul, J. P.; Chongsawangvirod, S.; Andrews, J. W.; Irene, E. A. *J. Electrochem. Soc.* **1990**, *137*, 234.
(28) Jellison, G. E., Jr. *J. Appl. Phys.* **1991**, *69*, 7627.
(29) Wang, Y.; Irene, E. A. *J. Vac. Sci. Technol. B* **2000**, *18*, 279.
(30) Saurel, O.; Cezanne, L.; Milon, A.; Tocanne, J. F.; Demange, P. *Biochemistry* **1998**, *37*, 1403.
(31) Hovis, J. S.; Boxer, S. G. *Langmuir* **2001**, *17*, 3400.

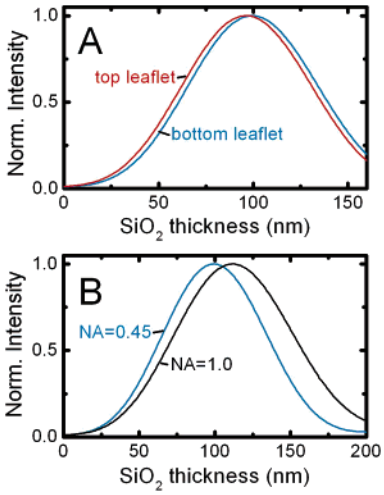

Figure 2. (A) Calculations of the normalized fluorescence intensity as a function of SiO_2 thickness for a DiI-containing supported membrane with different distributions of fluorophores assuming a 1.5 nm thick water layer. The red line and blue line correspond to the relative intensity of supported membranes on a FLIC chip containing DiI only in the upper leaflet ($d_2 = 3.69$ nm, $f_2 = 1$) and only in the bottom leaflet ($d_1 = 0.09$ nm, $f_1 = 1$), respectively. Other parameters in this calculation include NA = 0.45, $\gamma_{abs} = 76.5°$, $\gamma_{em} = 80°$. (B) Effect of varying the numerical aperture (NA = 0.45, blue line; NA = 1.0, black line) on the calculated fluorescence intensity as a function of SiO_2 thickness of a supported membrane with DiI only in the bottom leaflet. All other parameters are the same as in (A).

have developed an electromagnetic model that describes steady-state fluorescence near a multilayer interface that includes absorptive losses, nonradiative decay, and near-field losses. The equations derived by Lambacher and Fromherz[22] are more general cases of equations derived by Hellen and Axelrod,[32] Sullivan and Hall,[33] and Mertz[34] among others. A general discussion of the general principles of FLIC has been presented by Parthasarathy and Groves.[35] We use the model of Lambacher and Fromherz to model and fit FLIC data. The observed fluorescence intensity per unit time for a fluorophore near the FLIC chip surface, J, depends on the excitation rate of the fluorophore ($k_{ex,ill}$), the detection rate of emitted photons ($k_{em,det}$), the rate emitted by the fluorophore (k_{elmag}), and rate of de-excitation due to nonradiative processes:

$$J = \frac{k_{ex,ill} k_{em,det} / k_{fl}^{\infty}}{(k_{elmag}/k_{fl}^{\infty}) - 1 + \Phi_{fl}^{-1}} \quad (1)$$

where Φ_{fl} is the quantum yield of the fluorophore and k_{fl}^{∞} is the rate of fluorescence emission in the absence of the surface. The full expressions for $k_{ex,ill}$, $k_{em,det}$, and k_{elmag} can be found in the work of Lambacher and Fromherz[22], and we follow their notation. Because it occurs in the expressions for $k_{em,det}$ and k_{elmag}, k_{fl}^{∞} cancels out and need not be explicitly calculated. Equation 1 gives J in units of energy/s; however, since the fluorescence intensity in measured in counts/s, the data is fit to

$$J_{exp} = aJ \quad (2)$$

where a is simply a scaling factor that is constant for all the SiO_2 steps.

Because the value of d_{water} is determined by measuring the position of the DiI fluorophores relative to the SiO_2 surface, the fraction of fluorophores in the bottom and top leaflet of the membrane, f_1 and f_2, respectively, and their positions in the membrane, d_1 and d_2, respectively, (see Figure 1A) must be known. Alternatively, if d_{water}, f_1, and f_2 are known, then d_1 and d_2 can be determined. To fit for $d_{oligo-Alexa}$, the Alexa fluorophores are assumed to be uniformly located at a fixed distance away from the surface. If a calculated FLIC curve, generated using a

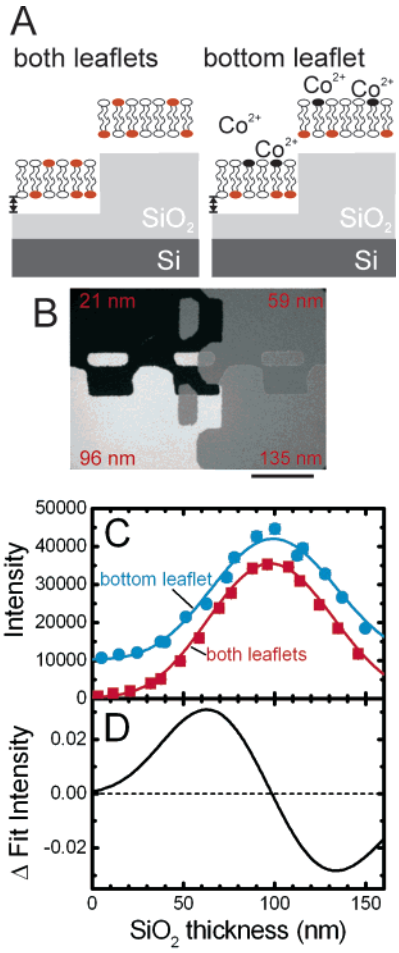

Figure 3. (A) Schematic diagram of DiI-containing egg PC supported membrane in the absence and presence of cobalt(II) chloride. In the absence of Co^{2+}, DiI fluorescence is emitted from positions in both leaflets of the supported membrane; addition of Co^{2+} quenches the DiI fluorescence in top leaflet of the supported membrane; thus, the detected fluorescence only originates from DiI fluorophores in the bottom leaflet. (B) Epi-fluorescence image of a DiI-containing supported membrane in the absence of Co^{2+} at the intersection of four SiO_2 steps of varying thicknesses as indicated on a FLIC chip. The puzzle-piece-shaped border between the SiO_2 steps is a result of the transparency photomask used to create the FLIC chip (see Materials and Methods). The scale bar is 100 μm. (C) Red squares and blue circles show the background-corrected fluorescence intensity as a function of SiO_2 for DiI-containing membranes in the absence and presence of Co^{2+}, respectively. For ease of comparison, the fluorescence intensity in the presence of Co^{2+} is offset vertically by 10 000 cts. The best fit for data in the absence of the Co^{2+}, corresponding to $d_{water} = 1.2 \pm 0.1$ nm, was determined using eq 2 and the appropriate distribution of DiI molecules ($d_1 = 0.09$ nm, $f_1 = 0.46$, $d_2 = 3.69$ nm, $f_2 = 0.54$) and is shown as a red line. The best fit for data in the presence of Co^{2+} corresponds to $d_1 = 0.2 \pm 0.2$ nm is shown as a blue line and was determined using eq 2 and $d_{water} = 1.3$ nm, respectively. (D) The difference between the best fit to the data for both leaflets (red line in C) and the best fit to the data for the bottom leaflet (blue line in C) as a function of SiO_2 thickness. The best fits were scaled to a magnitude of 1 at their maxima, so the units on the y axis are the fractional intensity difference.

(32) Hellen, E. H.; Axelrod, D. *J. Opt. Soc. Am. B: Opt. Phys.* **1987**, *4*, 337.
(33) Sullivan, K. G.; Hall, D. G. *J. Opt. Soc. Am. B: Opt. Phys.* **1997**, *14*, 1149.
(34) Mertz, J. *J. Opt. Soc. Am. B: Opt. Phys.* **2000**, *17*, 1906.
(35) Parthasarathy, R.; Groves, J. T. *Cell Biochem. Biophys.* **2004**, *41*, 391.

model with a distribution of fluorophores, is fit with a model that has all the fluorophores located at a single position, then the resulting best fit value for the single position model is approximately equal to the weighted average of the original distribution. Interference in the z direction is caused by the difference in path length between the incoming and reflected rays. This path length difference for any z position depends on the wavelength of light, its incidence angle relative to the surface normal (θ_{inc}), the refractive indices of the layer system, and the thickness of each layer. Therefore, eq 1 includes the relative contributions of the light wavelengths involved in excitation, emission, and detection. The range and relative contribution of θ_{inc}'s is given by the numerical aperture of the objective (NA) and the aperture function, which describes the intensity of excitation light as a function of θ_{inc}. The model of Lambacher and Fromherz assumes that the intensity is a constant for all θ_{inc}'s and compensates for this approximation (which is incorrect for most microscopes) by treating the NA as a free parameter.[22] For the narrow distribution of θ_{inc}'s used in these experiments, the aperture function is not expected to have a significant effect on the fitted value of d_{water} or $d_{oligo-Alexa}$, so the data were fit using the specified NA and treating the aperture function as a constant. The terms in eq 2 account for the dependence of the absorption probability on the angle between the absorption transition dipole moment and the direction of the excitation light electric field and the probability of emission along a given θ_{inc}'s given by the orientation of the emission transition dipole moment. The orientations of the absorption and emission transition dipole moments are described relative to the surface normal, γ_{abs} and γ_{em}.

The refractive indices of Si, SiO_2, and H_2O as a function of wavelength are taken from Palik.[36] As mentioned above, ellipsometric measurements show the SiO_2 refractive index to be a function of the SiO_2 thickness for very thin films; however, use of a more complex model of SiO_2 refractive index in the FLIC fitting routine did not significantly change the value of d_{water} or $d_{oligo-Alexa}$. The highly hydrated headgroup regions of the lipid bilayer were assumed to have the same refractive index as water and are thus treated as part of the aqueous layers. The refractive index of the hydrocarbon region of the membrane was taken to be 1.475, independent of wavelength. The thickness of the hydrocarbon region of a hydrated egg PC bilayer is 3.78 nm.[37,38] From fluorescence quenching studies of membrane probes that have a similar structure to DiI using the parallax method,[39] the DiI fluorophore is located 0.09 nm inside hydrocarbon region of the membrane. The absorption and emission spectra of DiI in methanol and Alexa 594 C_5 maleimide in water were obtained from the manufacturer. The quantum yield of Alexa 594 is approximately 0.55,[40] and the quantum yield of DiI is assumed to be 0.38 on the basis of the measured quantum yields of related compounds.[41,42] Following the analysis by Sund et al.,[43] the absorption and emission transition dipole moment of DiI are aligned 76.5° and 80°, respectively, relative to its conjugated bridge axis, that this axis is parallel to the membrane plane, and that the membrane is perfectly parallel to the SiO_2 surface, giving $\gamma_{abs} = 76.5°$ and $\gamma_{em} = 80°$. The absorption and emission transition dipole moments of Alexa 594 are assumed to be parallel on the basis of the measured limiting anisotropy ($r_o = 0.376$) of the structurally related Alexa 488 fluorophore.[44]

The output spectrum of the mercury arc lamp and the transmission spectra of the excitation filters, emission filters, and dichroic mirrors were obtained from the respective manufacturers. The numerical modeling codes used to produce the calculations and fits were written in Matlab.

Results and Discussion

Quantitative Determination of Water Layer Thickness and Resolution Test. Although the approach of Kiessling and Tamm inspired us to use FLIC to characterize the structure of supported membranes, here we refine the accuracy of the measurement of the thickness of the water layer, d_{water}, by characterizing the distribution of DiI fluorophores in the supported membrane and explicitly accounting for this distribution in the model used to fit the data. Although it is typically assumed that a fluorescent lipid probe is equally partitioned between the two leaflets of the supported membrane, recent results have shown that the distribution can be highly asymmetric for charged lipid probes.[45−47] As illustrated in Figure 2A, calculations of the same water layer thickness with different distributions of fluorophores give similar, yet distinguishable, FLIC curves. To a first approximation for our experimental conditions, the sum of the fitted water layer thickness (d_{water}) and the weighted average of the fluorophore position ($d_{fluoravg}$; $d_{fluoravg} = f_1d_1 + f_2d_2$), i.e. $d_{fluoravg} + d_{water}$, is constant for a given set of data. That is, if the value of $d_{fluoravg}$ used as a known parameter is increased by 1.0 nm, then the fitted d_{water} value will decrease by 1.0 nm. As we demonstrate in experiments discussed below, incorrect assumptions of fluorophore distribution yield incorrect measurements of d_{water}.

Additionally, we sought high-precision FLIC measurements and a quantitative demonstration of FLIC's z resolution. To accomplish this, the systematic error in intensities caused by inhomogeneous illumination across the field of view was eliminated by using larger SiO_2 steps and by comparing intensities at the same position within the field of view as described above (see Materials and Methods). We also chose to use smaller NA objectives to image supported membranes using FLIC.[35] Figure 2B shows calculations of the fluorescence intensity, normalized to 1 at the maximum intensity, as a function of SiO_2 thickness for a small 0.45 NA objective and for a large 1.0 NA objective. The variation in intensity is steeper for the small NA; since each θ_{inc} has an intensity maximum that occurs at a slightly different SiO_2 thickness, increasing the number of θ_{inc}'s broadens the FLIC curve. Assuming that the same signal-to-noise ratio can be produced with large NA and small NA objectives (a situation that is true for our experiments), the steeper FLIC curve associated with a smaller NA objective would provide higher precision z positions.[48]

Quenching experiments using cobalt(II) chloride were performed to determine the DiI distribution in egg PC supported membranes. Several observations indicate that 500 mM cobalt(II) chloride completely quenches only the fluorescence from DiI in the top leaflet, i.e., the leaflet furthest from the solid support. In the presence of 500

(36) Palik, E. D. *Handbook of Optical Constants of Solids*; Academic Press: New York, 1985; Vol. II.

(37) Simon, S. A.; Advani, S.; McIntosh, T. J. *Biophys. J.* **1995**, *69*, 1473.

(38) Balgavy, P.; Dubnickova, M.; Uhrikova, D.; Yaradaikin, S.; Kiselev, M.; Gordeliy, V. *Acta Phys. Slovaca* **1998**, *48*, 509.

(39) Kachel, K.; Asuncion-Punzalan, E.; London, E. *Biochim. Biophys. Acta* **1998**, *1374*, 63.

(40) Panchuk-Voloshina, N.; Haugland, R.; Bishop-Stewart, J.; Bhalgat, M.; Millard, P.; Mao, F.; Leung, W.; Haugland, R. *J. Histochem. Cytochem.* **1999**, *47*, 1179.

(41) Krieg, M.; Srichai, M. B.; Redmond, R. W. *Biochim. Biophys. Acta* **1993**, *1151*, 168.

(42) Sims, O. J.; Waggoner, A. S.; Wang, C. H.; Hoffmann, J. F. *Biochemistry* **1974**, *13*, 3315−3330.

(43) Sund, S. E.; Swanson, J. A.; Axelrod, D. *Biophys. J.* **1999**, *77*, 2266.

(44) Rusinova, E.; Tretyachenko-Ladokhina, V.; Vele, O.; Senear, D.; Ross, J. *Anal. Biochem.* **2002**, *308*, 18.

(45) Provencal, R. A.; Ruiz, J. D.; Parikh, A. N.; Shreve, A. P. *Biophys. J.* **2001**, *80*, 423A.

(46) Cobalt quenching of 1% Texas Red supported membranes formed by vesicle fusion shows that 70% of the Texas Red DHPE is in the top leaflet (data not shown).

(47) Crane, J. M.; Kiessling, V.; Tamm, L. K. *Langmuir* **2005** *21*, 1377.

(48) Varying the range of excitation θ_{inc}'s also modulates the period of interference pattern. This modulation of θ_{inc} provides a way of measuring the z position of a fluorescent object without the necessity of replicating it over many SiO_2 steps (Ajo-Franklin, C. M.; Ganesan, P. V.; Boxer, S. G. manuscript in preparation.)

mM cobalt(II) chloride, the steady-state DiI fluorescence from a solution of detergent−phospholipid micelles or from a DiI-containing supported monolayer is completely quenched (data not shown). Despite this relatively high concentration of cobalt(II) chloride required for complete quenching, vesicle and supported membrane experiments both suggest that only the DiI fluorophores accessible to bulk solution are quenched. Addition of 500 mM cobalt(II) chloride to 0.5 mol% DiI-containing 50-nm-diameter egg PC vesicles or egg PC glass-supported membranes results in immediate quenching of 60 ± 2% and 54 ± 4% of the steady-state fluorescence, respectively.[49] Addition of higher concentrations of cobalt(II) chloride did not result in increased quenching of the fluorescence. Taken together, we interpret these results as indicative of the percentage of DiI in the top leaflet: for intact vesicles, 60% ± 2% of the DiI is present in the outer leaflet, and 54% ± 4% of the DiI is in top leaflet for supported membranes. Although the negatively charged Texas Red probe is asymmetrically distributed in egg PC supported membranes such that the bulk of the fluorophores are in the upper leaflet,[45−47] i.e., the leaflet further away from the negatively charged SiO_2 surface, the positively charged DiI lipid is almost equally distributed between the two leaflets in egg PC supported membranes.[50]

With this information in hand, FLIC was used to determine d_{water}, the thickness of the water layer between the SiO_2 support and the bottom leaflet of the supported membrane. As shown in Figure 3B, vesicle fusion of egg PC vesicles containing 0.5 mol% DiI onto FLIC chips resulted in highly uniform fluorescence over a single SiO_2 step, and that intensity varied with the SiO_2 thickness. The data from these FLIC experiments have extremely good signal-to-noise ratios: the intensity standard deviation was ∼1% across a given SiO_2 step, while the maximum fluorescence intensity was ∼400% that of a glass-supported membrane of identical composition. Spot photobleaching demonstrated that there was no detectable immobile fraction and that the DiI lipids could freely diffuse from one SiO_2 step to the next (data not shown). Assuming the fluorophore distribution as previously determined, the FLIC data were fit with two free parameters as given by eq 2: a scaling parameter and d_{water}. Measurements of several supported membranes on different FLIC chips with sets of slightly varying SiO_2 step thicknesses yield $d_{water} = 1.3 \pm 0.2$ nm.

The precision in this measurement, 0.2 nm, is based on the variation in the fits across five different supported membranes. For a given data set of 16 intensities and SiO_2 thicknesses, the uncertainty in the best-fit value of d_{water} was quite small, i.e. standard deviation of ∼±0.02 nm. The best-fit values of d_{water} for 30 different regions taken from a single FLIC chip-supported membrane varied by ∼±0.05. As an additional indication of the accuracy of the model and parameters used to fit the data and as a quantitative demonstration of precision of the FLIC experiments, we performed FLIC on 0.5 mol% DiI-containing egg PC supported membranes in the presence of 500 mM cobalt(II) chloride, thus creating a situation in which only DiI molecules in the bottom leaflet fluoresce.[51] An example of the data from one such experiment is shown in Figure 3C. Using $d_{water} = 1.3$ nm, the FLIC curve can be fit to determine the position of the fluorophores in the bottom leaflet of the supported membrane, d_1. Over several experiments, the average fluorophore position agrees well with the measurement from parallex quenching experiments: $d_1 = 0.2 \pm 0.5$ nm[52] versus 0.09 ± 0.2 nm.[39] This agreement, based on FLIC data from both the quenched and unquenched DiI-containing membranes, provides additional confirmation that Co^{2+} quenches DiI only the top leaflet and of the water layer thickness.[54] The FLIC curve for a DiI-supported membrane in the presence of Co^{2+} is shifted to higher SiO_2 thicknesses relative to that of an identical membrane in the absence of Co^{2+}. This shift is small, corresponding to ∼2 nm, but significant and reproducible between multiple data sets with varying sets of SiO_2 step heights. Figure 3D highlights this

(49) In both the vesicle and supported-membrane quenching experiments, a slow decrease in fluorescence intensity, on the order of an additional 5% over 20 min, was observed. We attribute the observed gradual intensity decrease to slow traversal of the Co^{2+} across the lipid bilayer.

(50) While this work was being reviewed, Crane et al.[47] published a related study which assessed the fluorescent lipid distribution in supported membranes using FLIC. To determine fluorophore asymmetry, Crane et al. make two assumptions: (i) that 50% of the fluorophores is in each leaflet for symmetrically made Langmuir−Blodgett/Langmuir−Schaefer-supported membranes and (ii) that the water layer thickness is independent of the lipid composition. It would be valuable to confirm these two assumptions; the Co^{2+} quenching method provides a more direct method to determine lipid asymmetry, though it may not work for all lipids compositions and/or fluorophores. Although we measured the fluorophore distribution in supported membranes for a very limited set of cases, we find that different fluorophores can partition differently, and potentially asymmetrically, between the two leaflets of a supported membrane, which echoes the results of Crane et al. Likewise, we find that the structurally similar Rh−DPPE and Texas Red DHPE molecules seem to preferentially partition into the top (distal) leaflet. We find this asymmetry in a case where we would not necessarily expect asymmetry, i.e. supported membranes formed by vesicle fusion, suggesting that the asymmetry may be driven by interactions between surface charge on the glass support and charge in the fluorescently labeled lipids.

(51) We attempted to prepare supported membranes with DiI in only one leaflet by the monolayer-fusion technique;[52] however, control experiments revealed that DiI was present in both leaflets. Specifically, an egg PC monolayer was deposited on a FLIC chip by Langmuir Blodgett deposition, 0.5% DiI-containing egg PC vesicles were then added in buffer solution, and after a 3 min incubation, the surface was extensively rinsed with Millipore water. The resulting fluorescence was uniform and exhibited fully mobile two-dimensional diffusion. When the Co^{2+} quenching experiment was performed, only ∼50% of the fluorescence intensity was quenched. The commonly accepted mechanism of supported membrane formation by monolayer fusion predicts that all fluorescence would be quenched, i.e., all the DiI would be in the top leaflet. Additionally, we deposited a 2% 1-myristoyl-2-[6-[(7-nitro-2−1,3-benzoxadiazol-4-yl)amino]hexanoyl]-*sn*-glycero-3-phosphocholine (NBD-PC, Avanti Polar Lipids, Alabaster, AL)-containing egg PC monolayer by Langmuir−Blodgett deposition followed by monolayer fusion with unlabeled egg PC vesicles. Upon exposure of the supported membrane to Co^{2+}, ∼50% quenching of the NBD-PC was observed, as opposed the expected 0% quenching. The quenching experiments were done within ∼10 min of the vesicle addition. These experiments suggest that the lipid composition of the bottom leaflet of the supported membrane is composed of lipids from the initial monolayer and the vesicles, rather than composed of solely lipids from the initial monolayer. Our observation that the Langmuir−Blodgett/vesicle fusion method results in mixed rather than asymmetric supported membranes is in contrast to the results reported by Crane et al.[46] This difference is likely a reflection of differences in the materials (DiI or NBD-PC in egg PC vs Rh−DPPE in POPC) or the exact methods used in preparation of the supported membranes. In our rather limited experience, we find that different fluorophores in different lipid mixtures partition differently.

(52) Kalb, E.; Frey, S.; Tamm, L. K. *Biochim. Biophys. Acta* **1992**, *1103*, 307.

(53) The larger standard deviation in this measurement is likely due to systematic error from partial quenching of the bottom leaflet by slow leakage of Co^{2+} across the membrane over the course of a single experiment.

(54) If a significant proportion of the bottom leaflet fluorophores were quenched by the Co^{2+}, the values of f_1 and f_2 used in the fitting in the absence of Co^{2+} would be incorrect and the resulting best-fit value of d_{water} would be greater than the actual value. For example, if $f_1 = 0.56$ instead of $f_1 = 0.46$, the mean best-fit value of d_{water} would be 1.7 nm instead of 1.3 nm. Because the sum of $d_{fluoravg}$ and d_{water} is constant, an incorrectly large value of d_{water} obtained from FLIC of an unquenched DiI supported membrane would lead to a proportionally smaller value of d_1 in the quenched experiment. Note that the immediate quenching of a portion of the DiI in the bottom leaflet for the FLIC experiment in the presence of Co^{2+} would not affect the FLIC fitting, since all observed fluorescence would still be from the bottom leaflet, i.e., $f_1 = 1$.

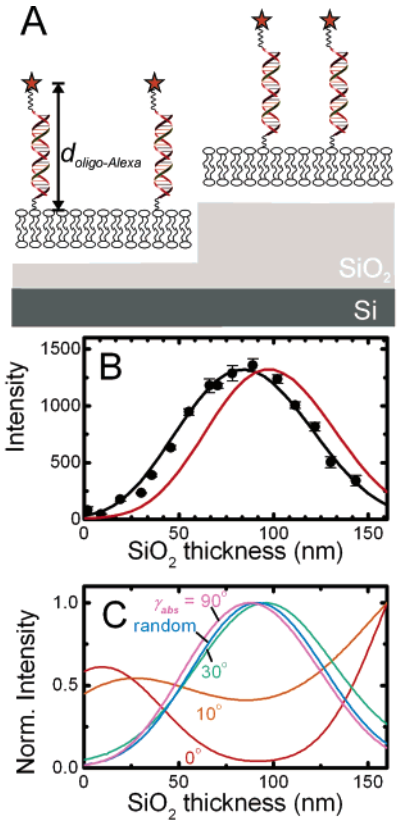

Figure 4. (A) Schematic diagram of Alexa-labeled oligonucleotide hybridized to a membrane-anchored oligonucleotides–lipid tether. (B) Fluorescence intensity as a function of SiO_2 thickness for Alexa-labeled oligonucleotide tethers (●). The solid black line corresponds the best fit using eq 2 with $d_{oligo-Alexa} = 12.2 \pm 0.2$ nm, assuming that the absorption and emission transition dipoles of the Alexa fluorophore are oriented parallel to the plane of the membrane. For reference, the red line shows the FLIC curve corresponding to a DiI-containing supported membrane in the absence of Co^{2+}. (C) Calculated effect of changing the orientation of the absorption transition moment orientation, γ_{abs}, relative to the membrane normal on the fluorescence intensity as a function of SiO_2 thickness for Alexa fluorophores located 10 nm from the top surface of the supported membrane. The emission transition moment is assumed to be parallel to the absorption moment.

difference by plotting the difference between the FLIC fits shown in Figure 3C, in which each fit was normalized to a maximum intensity of 1. If the two data sets were indistinguishable, the difference in normalized intensity would be a straight line at zero and the fitted value of d_1 would be close to 2.0 nm, i.e., the average position of the DiI when present in both leaflets. The absolute value of the difference in normalized intensity summed over all the steps (Σ |Δfit intensity|), i.e., the difference between the two data sets, is ~20% for the NA = 0.45 objective and would be ~4% for the NA = 1.0 objective. The signal-to-noise ratio for this experiment is ~1%, which strongly suggests that distinction between the both leaflet and bottom leaflet cases could not be made with a NA = 1.0 objective. These results demonstrate that the FLIC experiment is exquisitely sensitive to changes in fluorophore position and distribution in supported membranes, especially when low-NA objectives can be used.

Determination of Alexa-Labeled Oligonucleotide Tether Position. A schematic diagram of the Alexa-labeled oligonucleotide tethers is shown in Figure 4A. The duplex DNA consists of 24 base pairs, corresponding to an end-to-end distance of 7.8 nm. The 5′ end of the sense oligonucleotide is covalently coupled to the lipid headgroup by a disulfide bond and flexible linker region that is ~2 nm in length if fully extended. Likewise, the Alexa fluorophore is connected to the 5′ end of antisense oligonucleotide strand by a thioether bond and ~2.5 nm flexible linker. The oligonucleotide tethers bind sequence-specifically; a supported membrane displaying the sense oligonucleotide binds the Alexa-labeled antisense oligonucleotide strand but not noncomplementary Alexa-labeled oligonucleotides (data not shown). The Alexa-labeled oligonucleotide tethers diffuse freely in two dimensions with a diffusion coefficient on the order of ~1 $\mu m^2/s$, and upon application of an electric field parallel to the surface, they move toward the positive electrode (data not shown). A combination of absorption spectroscopy to measure the lipid concentration and fluorimetry to measure the concentration of Alexa-labeled tethered oligonucleotides was used to measure the density of displayed oligonucleotides as ~1 or 2 per vesicle (data not shown). Thus, the oligonucleotide-modified lipid density corresponds to approximately 0.01 mol% of the supported membrane or 2 tethered oligonucleotides per square micrometer.

An example of FLIC data for the Alexa-labeled oligonucleotide tethers is shown in Figure 4B. For comparison, the FLIC curve for a supported membrane with DiI in both leaflets is shown as a solid red line. The intensity maximum occurs at significantly smaller SiO_2 thicknesses for the Alexa-labeled oligonucleotide tethers in comparison to the DiI-supported membrane, suggesting that the Alexa fluorophore is displaced further from the SiO_2 surface. Although anisotropy measurement of related compounds suggest that the absorption and emission transition dipole moment of Alexa fluorophore are nearly collinear,[43] there is no independent information on the orientation of transition dipole moments of Alexa fluorophore relative to the surface.[55] This uncertainty in the orientation complicates fitting the FLIC data.

For a population of Alexa fluorophores located a fixed distance from the supported membrane surface, the shape and position of the intensity maximum of the FLIC curve changes with the orientation of their absorption transition dipoles relative to the surface. Figure 4C shows several calculated FLIC curves corresponding to different fluorophore orientations in which the fluorophore is located 10 nm from the membrane surface and each curve is normalized to have a maximum intensity of 1. For $\gamma_{abs} = \gamma_{em} < \sim 30°$, the shape of the calculated FLIC curves are incompatible with the data in Figure 4B and the fact that the Alexa fluorophores can be at most ~12.5 nm from the surface. However, for $\gamma_{abs} = \gamma_{em}$ ranging from 30° to 90°, the shape of the FLIC curves are similar to the data shown in Figure 4B; the main difference between these normalized curves is the shift of the intensity maximum position to larger SiO_2 thickness with decreasing γ_{abs}. To bound the possible range of values for $d_{oligo-Alexa}$, the data were fit separately with two models assuming a single fixed orientation corresponding to $\gamma_{abs} = 90°$ or $\gamma_{abs} = 30°$, giving $d_{oligo-Alexa}$ of 11.1 ± 2.2 and 17.3 ± 2.2 nm, respectively. The sum of the residuals and the sum of the square of the residuals for the fits are greater for the $\gamma_{abs} = 30°$ model than the $\gamma_{abs} = 90°$ model. A more realistic model for the Alexa-labeled oligonucleotide tethers would include a

(55) A fluorescence polarization experiment could be used to determine the average orientation of the Alexa 594 fluorophore relative to the surface normal. The surface coverage of fluorophores is on the order of 2 per square micrometer, so attaining sufficient signal-to-noise in such an experiment with our current setup would be extremely challenging.

distribution of orientations rather than a single orientation. Fitting the data to a model that assumes the Alexa fluorophore is randomly oriented yields $d_{\text{oligo-Alexa}} = 14.1 \pm 1.8$ nm; the residuals and sum of the square of the residuals in this case are approximately the same as those in the $\gamma_{\text{abs}} = 90°$ model. If the linkers associated with the Alexa-labeled oligonucleotide tether are fully extended and the axis of the duplex DNA is oriented normal to the surface, $d_{\text{oligo-Alexa}}$ would be its maximum possible value, ~12.5 nm. Therefore, these results strongly suggest that the Alexa fluorophore is separated from the surface by close to the maximal distance. That the oligonucleotide tether is oriented nearly normal to the membrane surface, despite the presence of a relatively long and flexible linker between the 5′ end and the lipid headgroup, is interesting. It is possible that this orientation results from repulsion between the highly negatively charged duplex DNA and remaining ~0.49 mol% unreacted and negatively charged N-PDP-PE lipids. It is observed that vesicles displaying noncomplementary oligonucleotides do not bind to the supported membrane, suggesting that there is not a strong attractive net force between these vesicles and the supported membrane. Taking these observations together, we suggest that the tethered vesicles are separated from the underlying supported membrane by close to the full oligonucleotide tether length.

Conclusions

In conclusion, we have measured the water layer thickness underlying supported egg PC membranes as 1.3 ± 0.2 nm. This result closely agrees with measurements of the water layer thickness underlying phosphatidylcholine bilayers using NMR[10] (1.7 ± 0.5 nm) and using FLIC[8] (1.7 ± 1.0 nm) but is a more precise measurement. FLIC measurements of egg PC supported membranes in which fluorescence was emitted only from the bottom leaflet confirmed the accuracy of this measurement and quantitatively demonstrated the ability to distinguish fluorophores separated by ~1.9 nm. Additionally, the distal 5′ end of the oligonucleotide tethers is separated from the supported membrane by close to the maximal distance.

Importantly, this set of experiments provides a straightforward resolution test and calibration standard for other high-z-resolution fluorescence microscopies. For these experiments, a small NA objective was used to increase the maximum resolution attainable with FLIC. For samples with more limited fluorescence intensities, use of a small NA objective is not desirable. Another approach to sharpen the interference pattern without decreasing the signal-to-noise ratio is to restrict the excitation θ_{inc}'s, yet use the full NA of the objective to maximize the ratio of detected/emitted photons. This can be accomplished by closing the aperture diaphragm down to a small but known size, restricting the excitation θ_{inc}'s to near 0°.[48] Taken together, these results reinforce the value of using FLIC to characterize fluorescent structures at and near membranes.

Acknowledgment. We acknowledge Dan Huh for his important contributions to the fabrication of the FLIC chips used in this work and Lisa Hwang for her help with the monolayer-fusion experiments.[51] This work was supported in part by grants from the NSF Biophysics Program and NIH Grant No. GM069630. Facilities of the NSF MRSEC Center on Polymer Interfaces and Macromolecular Assemblies (CPIMA) are gratefully acknowledged.

LA0468388